Supplementary Information

Light-activated Film Diffractive Optical Elements Enabling Diversified Optical Field Modulation

Ning Shen (沈柠)[1, 2], Honglong Hu (胡宏龙)[1, 3], Zhaoyi Wang (王兆亿)[1], Yuxing Zhan (占宇星)[1, 2], Conglong Yuan (袁丛龙)[1, 3]*and Zhigang Zheng (郑致刚)[1, 2]

[1] School of Physics, East China University of Science and Technology, Shanghai 200237, China

[2] School of Materials Science and Engineering, East China University of Science and Technology, Shanghai 200237, China

[3] School of Chemistry and Molecular Engineering, East China University of Science and Technology, Shanghai 200237, China

*Corresponding author: conglongyuan@ecust.edu.cn

Section S1

Preparation of the liquid crystal (LC) geometric phase-based DOEs: A glass substrate, which was ultrasonically bathed and UV–ozone cleaned and coated with photoalignment agent SD1 (from Dai-Nippon Ink and Chemicals), can be patterned by a Digital Mirror Device (DMD). The reactive monomers mixture solution (OCM-A0, T_i=75 °C, Δn_{633}=0.148, Raito Materials) was spin-coated on the treated glass substrate. The concentration and spin-coating rate of different half-wave conditions are shown in Table S1. The liquid crystal monomer which was coated on the glass substrate was heated at 80 °C to remove residual solvent, and then slowly cooled down to room temperature. Following this, photopolymerization was carried out under 365 nm (15 mW·cm^{-2}) light for a duration of 2 min. The spin-coating of reactive monomers and the UV polymerization were repeated twice to achieve the half-wave condition.

Preparation of the light-activated LCP film: The LC cell, which contains two glass substrates coated with photoalignment agent SD1, was uniformly alignment by 365 nm linearly polarized light. The cell gap was controlled by 40 μm spacers. The reactive monomers mixture (OCM-A0) was filled into the front part of the LC cell by capillary force in its isotropic phase at 80 °C, and then slowly cooled down to room temperature. It is worth noting that a gap should be left at the LC cell injection port for subsequent mixture filling. Photopolymerization was carried out under 365 nm (15 mW·cm^{-2}) light for a duration of 4 min. The azobenzene derivative 2Azo was employed for the light-activation of the LCP film, whose molecular structure and absorption spectra are shown in Fig. S2. A LC mixture containing of 87 wt% reactive monomers mixture (OCM-A0), 10 wt% of 2Azo (4,4'-bis[6-(acryloyloxy) hexyloxy]azobenz, Accela) and 3 wt% of photoinitiator Irgacure 784 (from Perfemiker) was prepared to fabricate the light-activated LCP film. The mixture was homogeneously mixed with dichloromethane (from General-Reagent) in a vial at 80 °C for about 1.5 hours. The LC mixture was filled into the LC cell by capillary force in its isotropic phase at 80 °C, and then slowly cooled down to 50 °C. Following this, photopolymerization was carried out under 532 nm light for a duration of 20 min. The light-activated LCP film (~ 40 μm) was then harvested from the LC cell after ultrasound.

Preparation of the light-activated FDOEs: The LC geometric phase-based DOE was assembled with the light-activated LCP film by OCA optical tape. Then the light-activated FDOE (~ 65 μm) was harvested from the glass substrate after ultrasound.

Table S1 Spin-coating conditions of different half-wave conditions

Wavelength	Concentration of the reactive monomers	Spin-coating rate	Thickness of the DOEs
457 nm	25%	5400 rpm	1.54 μm
532 nm	25%	2500 rpm	1.80 μm
633 nm	30%	2700 rpm	2.14 μm

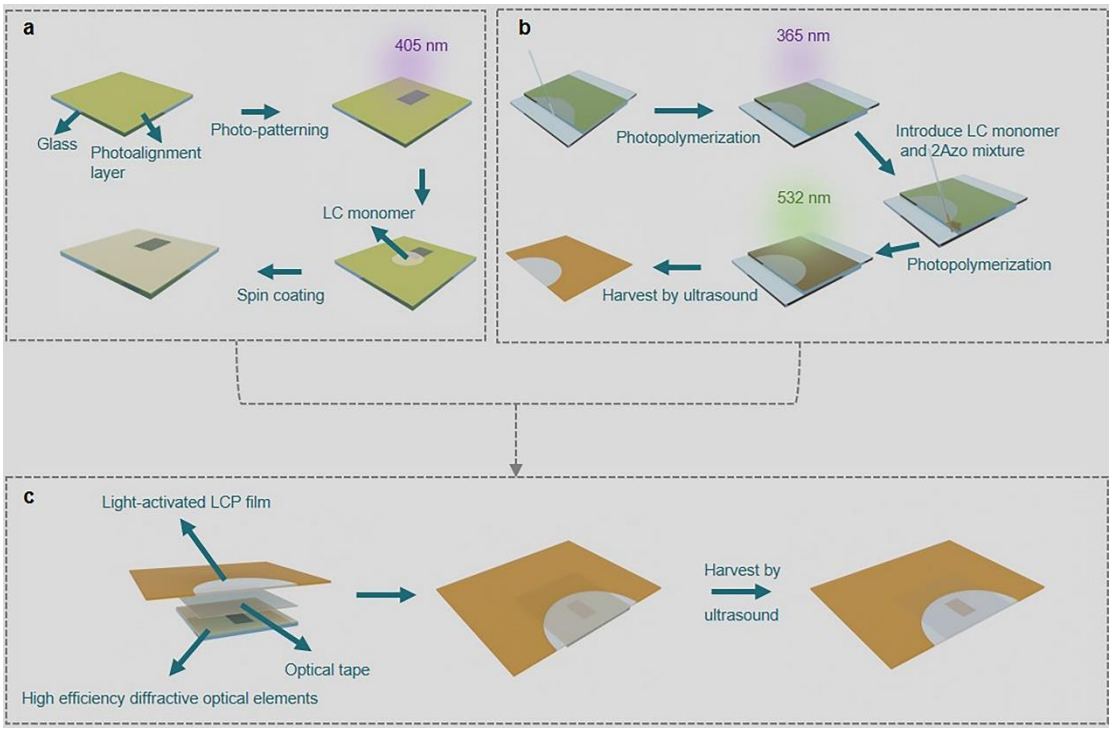

Fig. S1 (a) Diagram of preparation process of LC geometric phase-based DOEs. (b) Diagram of preparation process of light-activated LCP films. (c) Diagram of preparation process of light-activated FDOEs.

The light-activated FDOE is fabricated by integrating the LC geometric phase-based DOEs with light-activated LCP films. It is crucial to highlight that, in order to address the constraints imposed by azobenzene derivatives on the incident light wavelength, the light-activated LCP film is divided into two segments: a light-transmitting part facilitating the transmission of diffracted light from the DOE, and a photodeformable section that alters the position of the DOE relative to the incident light. This strategic partitioning ensures efficient modulation of the optical field while accommodating the specific requirements of the incident light.

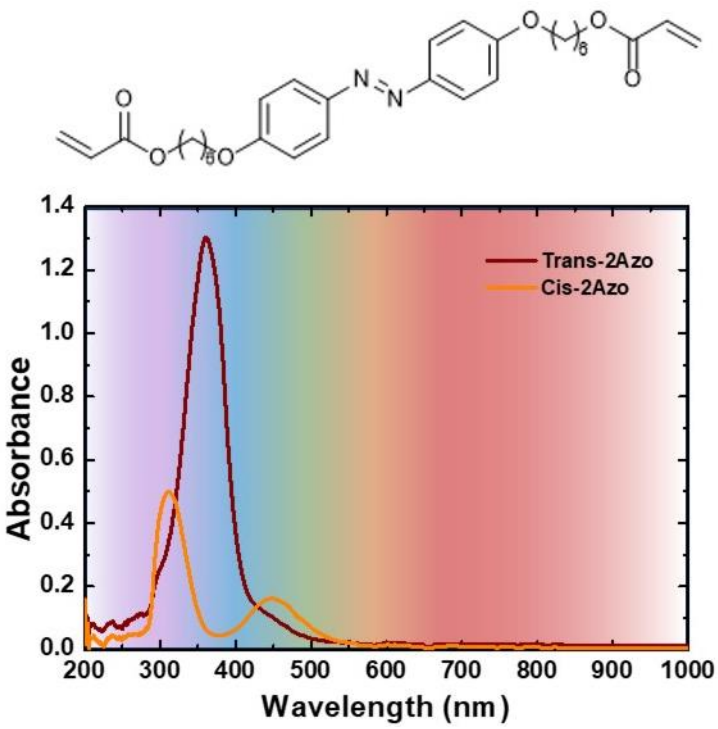

Fig. S2 The molecular structure and absorption spectra of the azobenzene derivative 2Azo.

The top half of Fig. S2 shows the structure of the 2Azo, in which the azophenyl group can achieve a reversible *trans*-to-*cis* photoisomerization to bring about the deformation of the LCP film. Additionally, the molecule, which features double bonds at both ends, is capable of being copolymerized with the LC monomers to prevent a degradation of the film's mechanical properties. The bottom half of Fig. S2 shows the absorption spectra of *trans*-2Azo and *cis*-2Azo, which have no absorption at a wavelength greater than 580 nm.

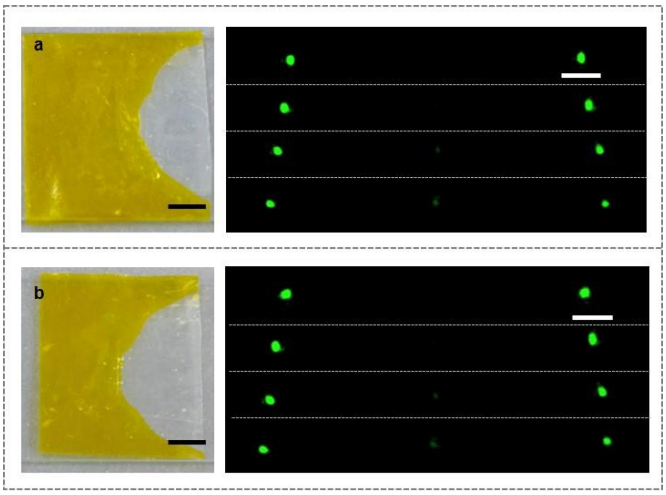

Fig. S3 Optical characterization of the film polarization grating with different areas of the light-transmitting section. The scale bar is 5 mm.

Since the proposed FDOE can be light-activated and exhibits excellent optical performance, two conditions must to be met for the area of the light-transmitting section: it should not affect the bending of the LCP film and must completely cover the patterned microstructure of the DOE. On the basis of satisfying these two conditions, the area of the light-transmitting section in the LCP film does not affect the optical performance of FDOEs. As illustrated in Fig. S3, the light-transmitting area of the FDOE in Fig. S3b is significantly larger than that in Fig. S3a, yet their optical performance remains essentially the same, as shown on the right side of Fig. S3.

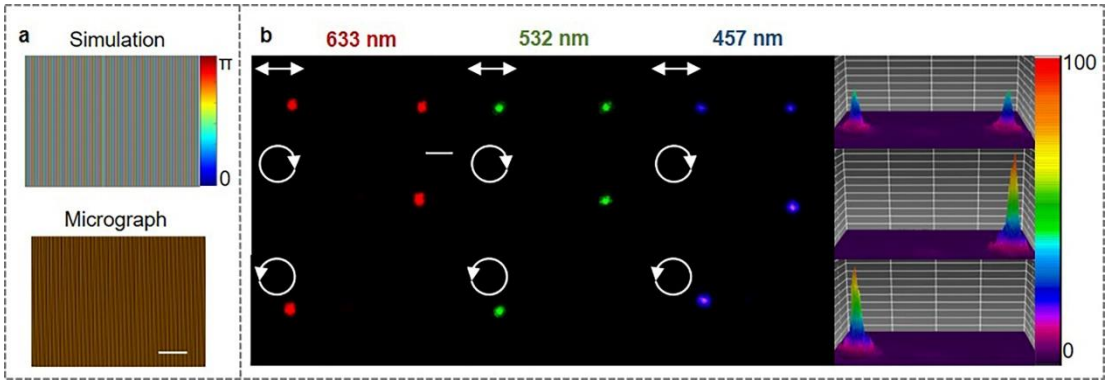

Fig. S4 Characterization of light-activated film polarization grating (PG) with a period of 20 μm. (a) Phase distribution (top) and microscopy texture (down) of the PG. The scale bar is 200 μm. (b) The diffraction spot images of the PG at 633 nm, 532 nm, and 457 nm half-wave conditions. The arrows represent the polarization states of the incident light, and the clockwise/counterclockwise circles represent right-handed/left-handed circularly polarized light. The diffraction spots are captured at 15 cm, and the image of the corresponding intensity distribution is shown on the far right. The scale bar is 1 mm.

The fabricated PG demonstrates exceptional optical performance with the incident light of varying polarization states and wavelengths under the corresponding half-wave condition.

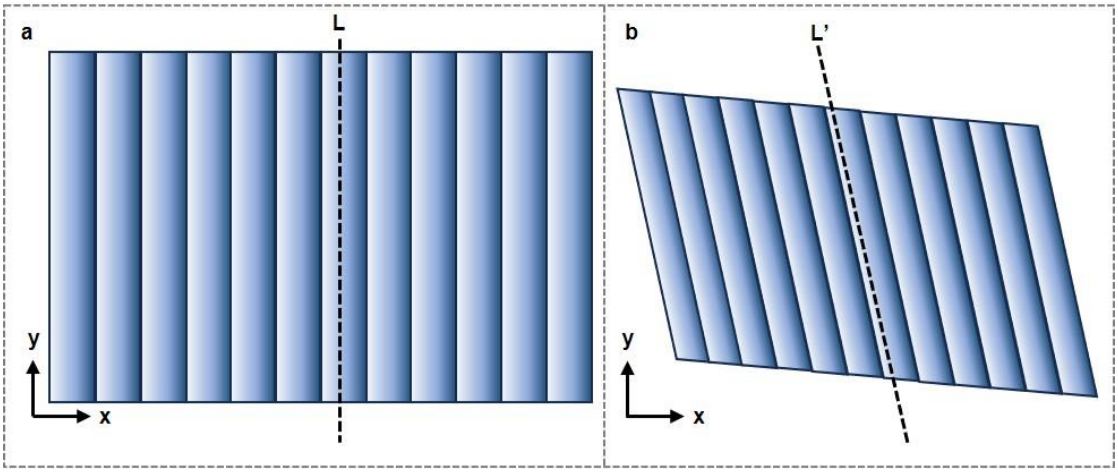

Fig. S5 (a) Diagram of periodic distribution of the PG without bending. (b) Projection of PG in the vertical plane of incident light after bending.

When incident light is vertically incident on the film polarization grating (PG), the periodic distribution of the PG, with its axis L parallel to the y-axis, is illustrated in Fig. S5a. Conversely, when the film PG is bent along the diagonal, the incident light changes to oblique incidence. The PG then deviates diagonally from the vertical plane of the incident light, causing the rectangular PG in Fig. S5a to be projected as a parallelogram PG onto the vertical plane of the incident light, as shown in Fig. S5b, which is equivalent to the incident light vertically incident the parallelogram PG structure, whose axis L' is rotated relative to the y-axis. Consequently, the 2D beam steering has happened.

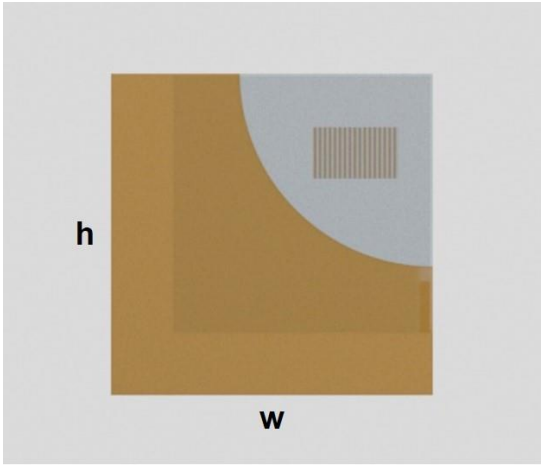

Fig. S6 The diagram of the aspect ratio of the light-activated film PG (w/h).

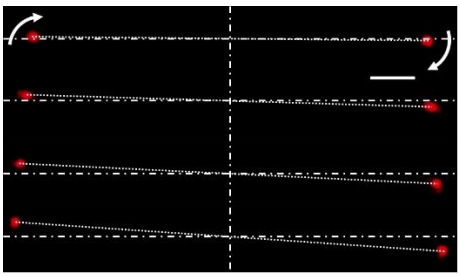

Fig. S7 The clockwise rotation of the ±1st order diffraction spots in 2D beam steering with PG locating in the lower right corner of the light-activated LCP film. The scale bar is 5 mm.

The clockwise 2D beam steering occurs when the PG is located in the upper left or lower right corner of the light-activated LCP film.

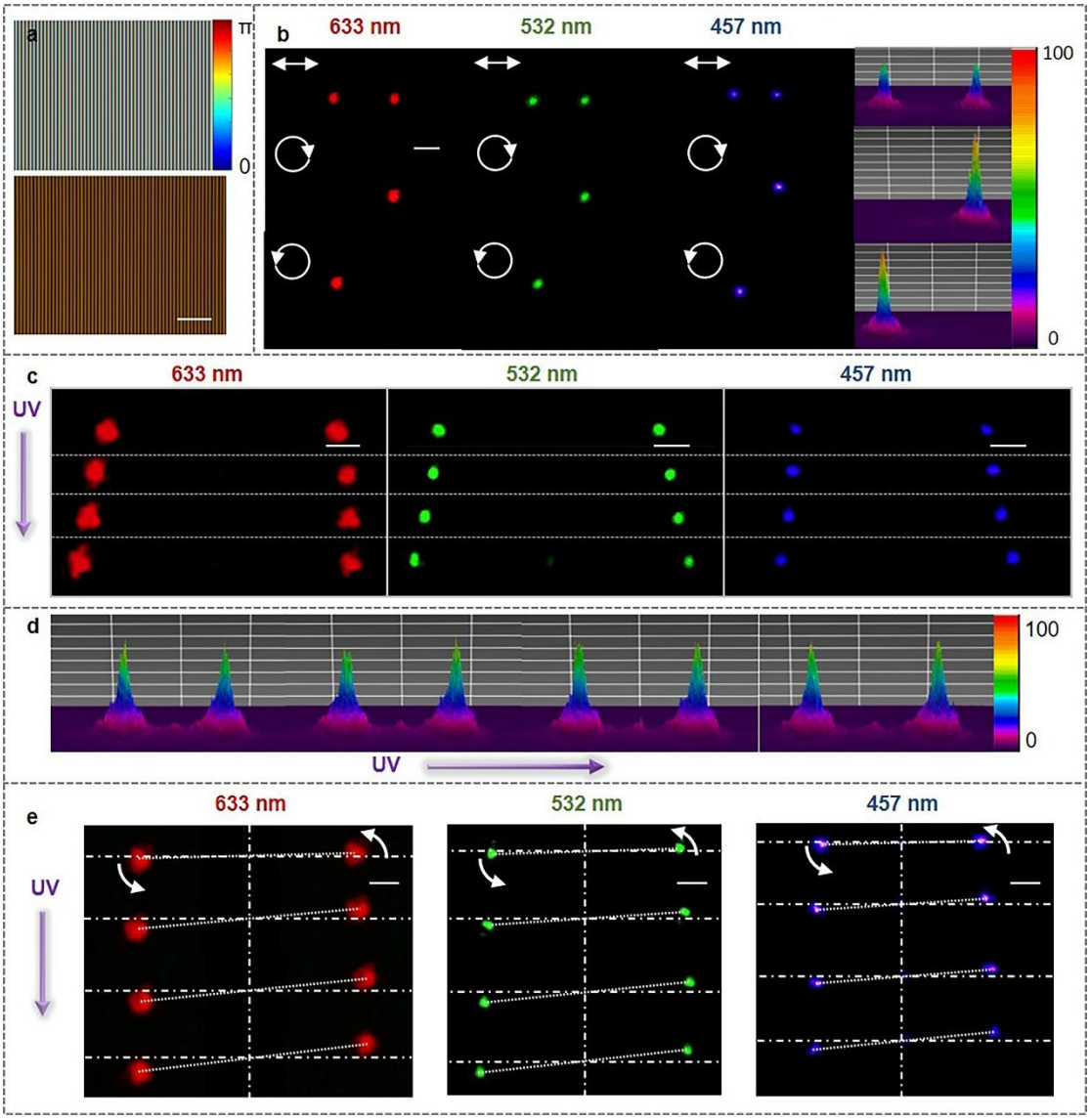

Fig. S8 Characterization of light-activated film PG with the period of 40 μm. (a) Phase distribution (top) and microscopy texture (down) of the PG. The scale bar is 200 μm. (b) The diffraction spots images of the PG at 633 nm, 532 nm, and 457 nm half-wave conditions. The arrows represent the polarization states of the incident light, and the clockwise/counterclockwise circles represent right-handed/left-handed circularly polarized light. The diffraction spots are captured at 15 cm, and the image of the corresponding intensity distribution is shown on the far right. The scale bar is 1 mm. (c) Images of the $\pm 1^{st}$ order diffraction spots migrating in one-dimensional (1D) direction with UV light irradiation. From top to bottom, the UV light is irradiated 0 s, 5 s, 10 s, and 15 s. The scale bar is 3 mm. (d) Images of intensity distribution during the $\pm 1^{st}$ order diffraction spots migrating in 1D direction. (e) Images of the $\pm 1^{st}$ order diffraction spots rotating in two-dimensional (2D) plane with UV light irradiation. From top to bottom, the UV light is irradiated 0 s, 5 s, 10 s, and 15 s. The scale bar is 3 mm. The incident light is linearly polarized with wavelengths of 633 nm, 532 nm, and 457 nm, respectively. The diffraction spots are captured at 70 cm.

Similar to the 20 μm-period light-activated film PG, the 40 μm-period light-activated film PG is also exhibited 1D diffraction angle tuning and 2D rotational, but the extent of beam steering is smaller than the 20 μm-period one.

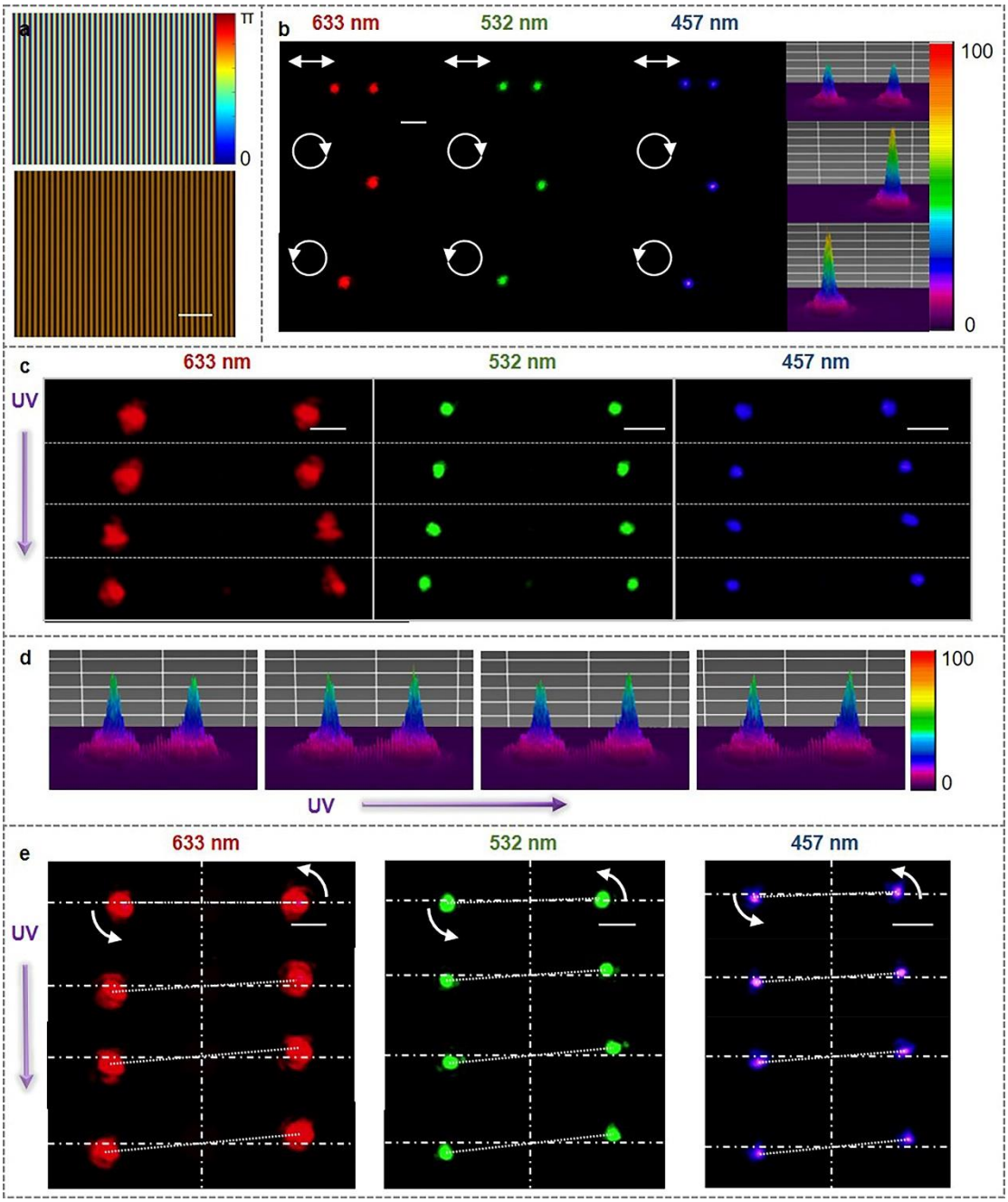

Fig. S9 Characterization of light-activated film PG with the period of 60 μm. (a) Phase distribution (top) and microscopy texture (down) of the PG. The scale bar is 200 μm. (b) The diffraction spots images of the PG at 633 nm, 532 nm, and 457 nm half-wave conditions. The arrows represent the polarization states of the incident light, and the clockwise/counterclockwise circles represent right-handed/left-handed circularly polarized light. The diffraction spots are captured at 15 cm, and the image of the corresponding intensity distribution is shown on the far right. The scale bar is 1 mm. (c) Images of the $\pm 1^{st}$ order diffraction spots migrating in 1D direction with the UV light irradiation. From top to bottom, the UV light is irradiated 0 s, 5 s, 10 s, and 15 s. The scale bar is 3 mm. (d) Images of intensity distribution during the $\pm 1^{st}$ order diffraction spots migrating in 1D direction. (e) Images of the $\pm 1^{st}$ order diffraction spots rotating in 2D plane with the UV light irradiation. From top to bottom, the UV light is irradiated 0 s, 5 s, 10 s, and 15 s. The scale bar is 3 mm. The incident light is linearly polarized with wavelengths of 633 nm, 532 nm, and 457 nm, respectively. The diffraction spots are captured at 70 cm.

Likewise, akin to both the 20 μm-period and 40 μm-period light-activated film PG, the 60 μm-period light-activated film PG is also showcased the capabilities of 1D diffraction angle tuning and 2D rotational. Nevertheless, its extent of beam steering is smaller than both the 20 μm-period and 40 μm-period one.

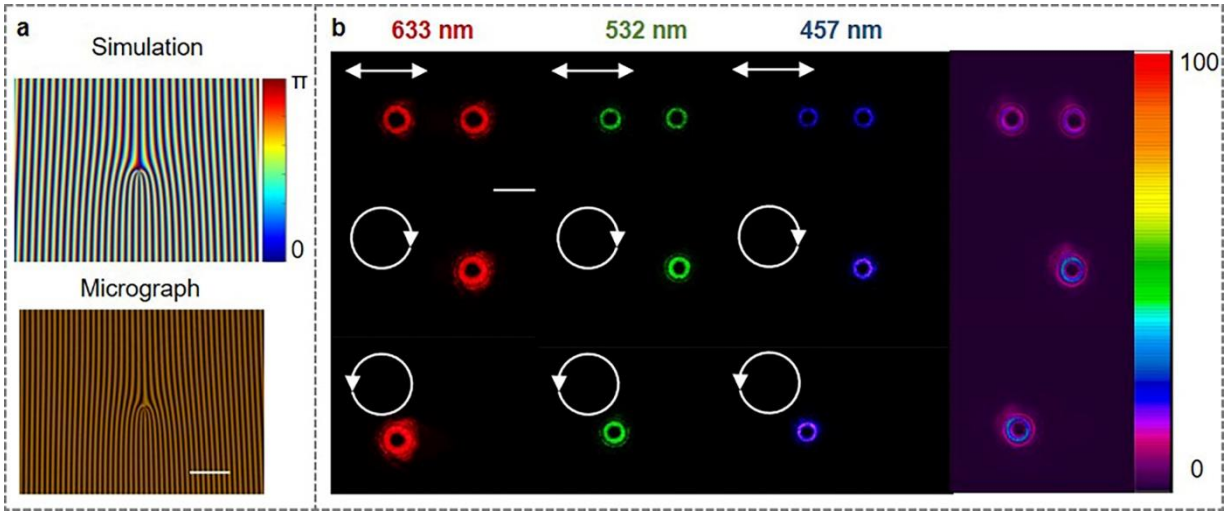

Fig. S10 Characterization of light-activated film fork polarization grating (FPG) with the period of 50 μm and the topological charge of +2. (a) Phase distribution (top) and microscopy texture (down) of the FPG. The scale bar is 200 μm. (b) The diffraction spots images of the FPG at 633 nm, 532 nm, and 457 nm half-wave conditions. The arrows represent the polarization states of the incident light, and the clockwise/counterclockwise circles represent right-handed/left-handed circularly polarized light. The diffraction spots are captured at 15 cm, and the image of the corresponding intensity distribution is shown on the far right. The scale bar is 1 mm.

The fabricated FPG demonstrates exceptional optical performance with the incident light of varying polarization states and wavelengths under the corresponding half-wave condition.

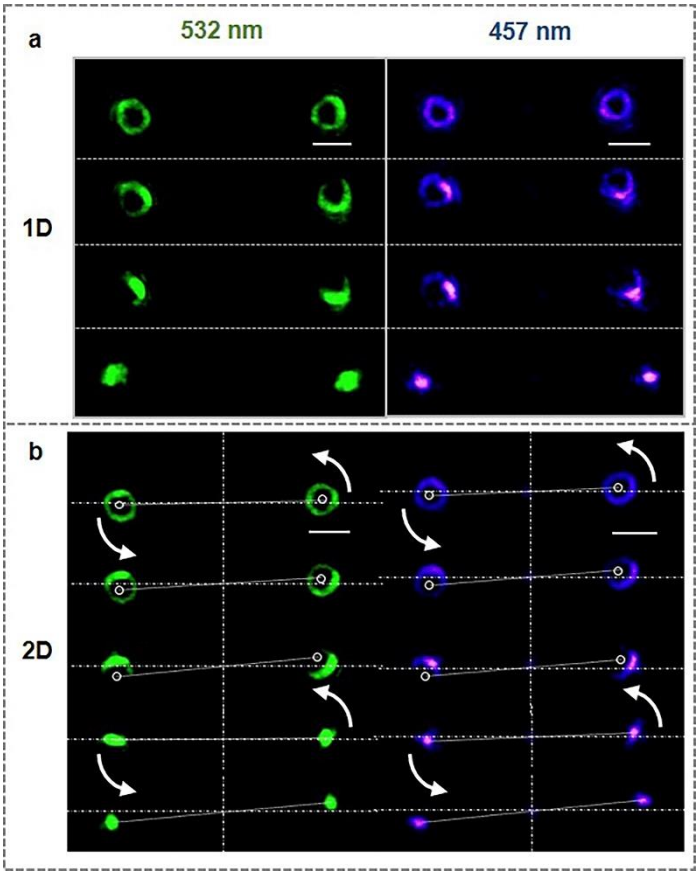

Fig. S11 Characterization of light-activated film FPG with the period of 50 μm and the topological charge of +2. (a) Images of the ±1st diffracted order switching between vortex light and Gaussian light under UV light irradiation based on the x-axis bending light-activated film FPG. From top to bottom, the UV light is irradiated at 0, 5, 10, and 15 s. The scale bar is 3 mm. (b) Images of the ±1st diffracted order switching between vortex light and Gaussian light under UV light irradiation based on the diagonal bending light-activated film FPG. From top to bottom, the UV light is irradiated 0 s, 4 s, 8 s, 12 s, 15 s. The scale bar is 3 mm. The incident light is linearly polarized with wavelengths of 532 nm and 457 nm. The diffraction spots are captured at 70 cm.

We demonstrate that the 1D and 2D structured optical field modulation behavior of the light-activated film FPG remains consistent across various incident light wavelengths, offering great latitude in the design of the film FPG.

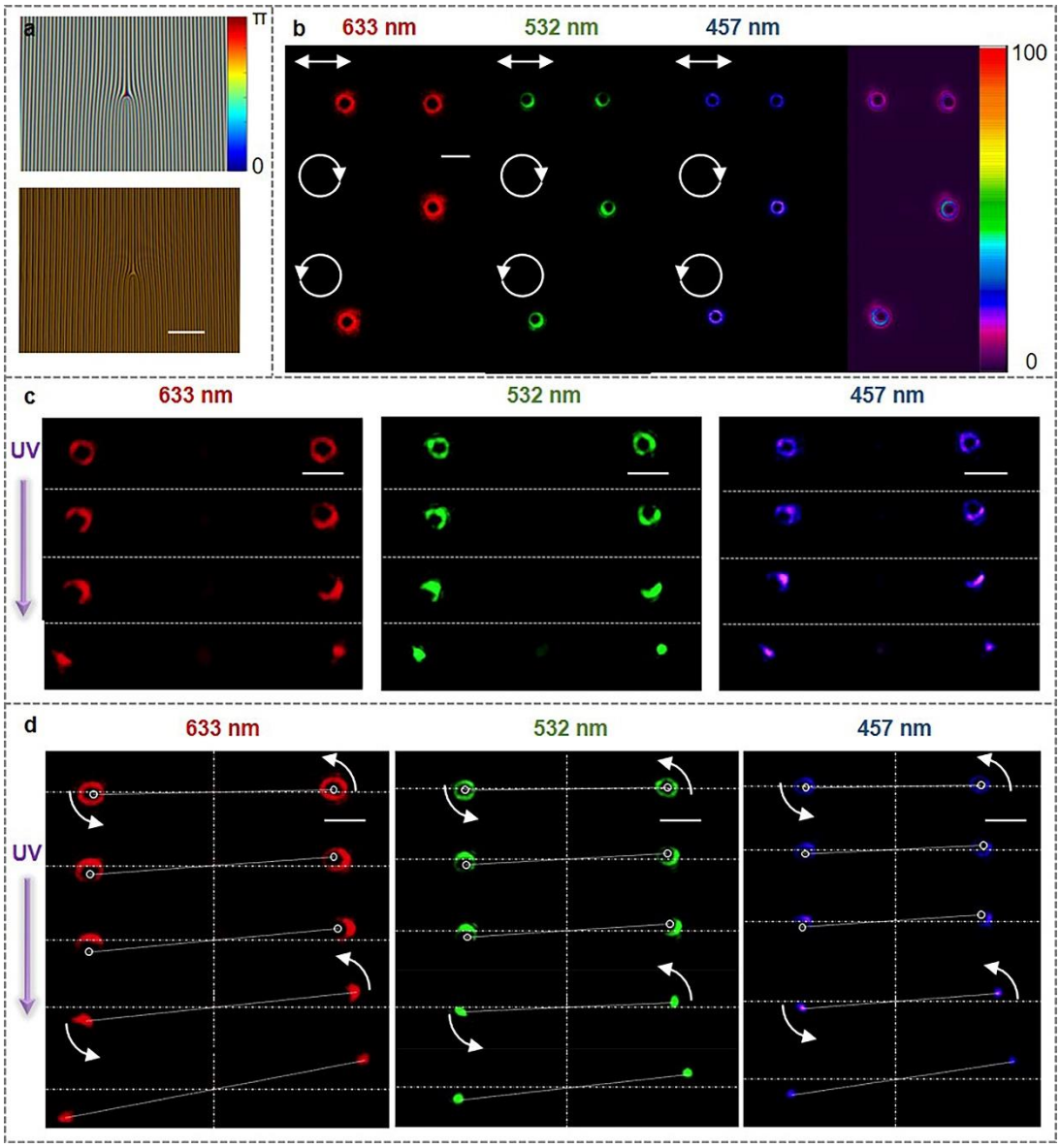

Fig. S12 Characterization of light-activated film FPG with the period of 30 μm and the topological charge of +2. (a) Phase distribution (top) and microscopy texture (down) of the FPG. The scale bar is 200 μm. (b) The diffraction spot images of the FPG at 633 nm, 532 nm, and 457 nm half-wave conditions. The arrows represent the polarization states of the incident light, and the clockwise/counterclockwise circles represent right-handed/left-handed circularly polarized light. The diffraction spots are captured at 15 cm, and the image of the corresponding intensity distribution is shown on the far right. The scale bar is 1 mm. (c) Images of the $\pm1^{st}$ diffracted order switching between vortex light and Gaussian light under UV light irradiation based on the x-axis bending light-activated film FPG. From top to bottom, the UV light is irradiated at 0, 5, 10, and 15 s. The scale bar is 5 mm. (d) Images of the $\pm1^{st}$ diffracted order switching between vortex light and Gaussian light under UV light irradiation based on the diagonal bending light-activated film FPG. From top to bottom, the UV light is irradiated 0 s, 4 s, 8 s, 12 s, 15 s. The scale bar is 5 mm. The incident light is linearly polarized with wavelengths of 633 nm, 532 nm, and 457 nm, respectively. The diffraction spots are captured at 70 cm.

Similar to the light-activated film FPG with a period of 50 μm and a topological charge of +2, the light-activated film FPG with a period of 30 μm and a topological charge of +2 is also demonstrated the reversible switching between $\pm1^{st}$ order vortex light and Gaussian light.

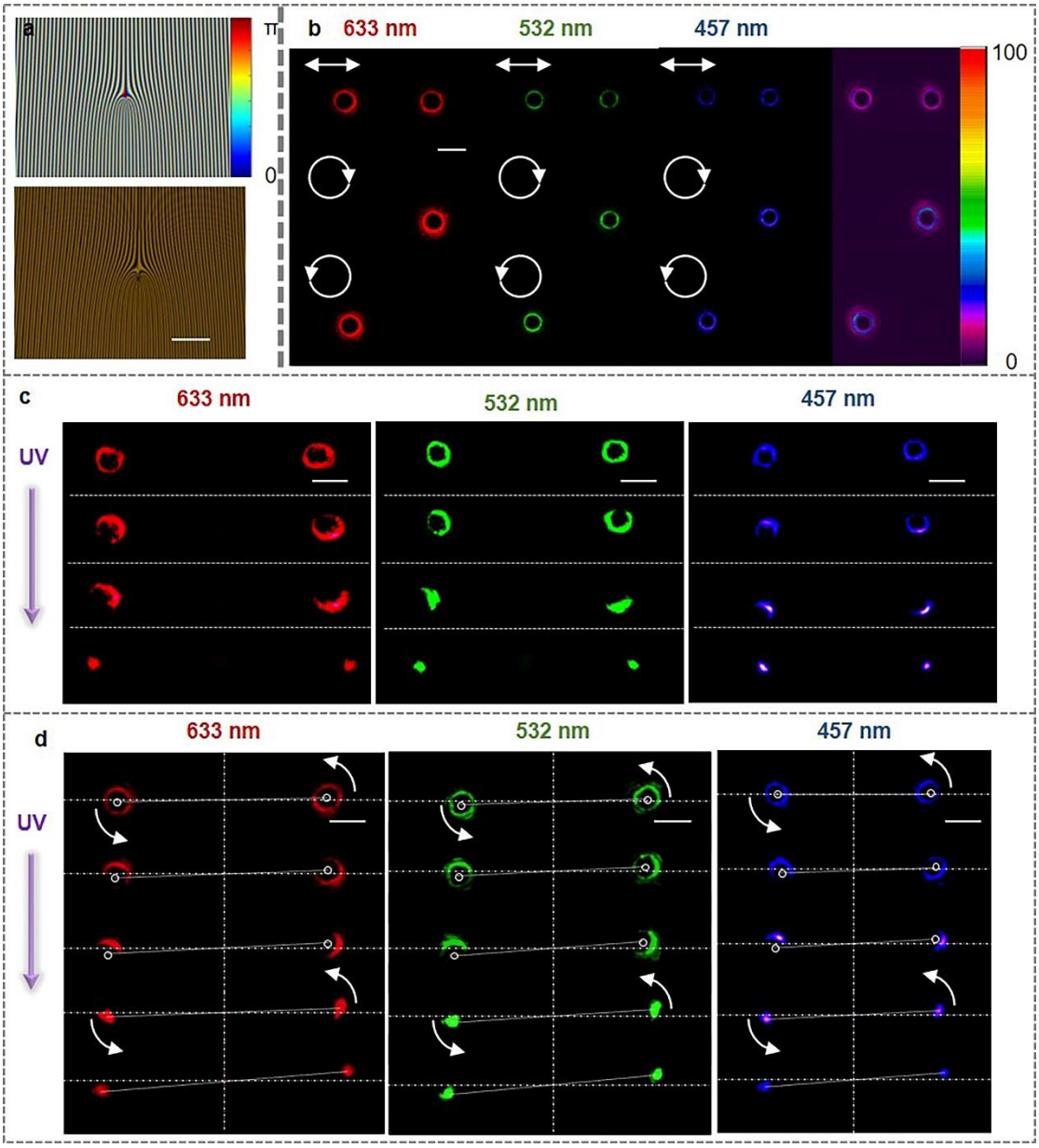

Fig. S13 Characterization of light-activated film FPG with the period of 30 μm and the topological charge of +4. (a) Phase distribution (top) and microscopy texture (down) of the FPGs. The scale bar is 200 μm. (b) The diffraction spot images of the FPG at 633 nm, 532 nm, and 457 nm half-wave conditions. The arrows represent the polarization states of the incident light, and the clockwise/counterclockwise circles represent right-handed/left-handed circularly polarized light. The diffraction spots are captured at 15 cm, and the image of the corresponding intensity distribution is shown on the far right. The scale bar is 1 mm. (c) Images of the $\pm1^{st}$ diffracted order switching between vortex light and Gaussian light under UV light irradiation based on the x-axis bending light-activated film FPG. From top to bottom, the UV light is irradiated at 0, 5, 10, and 15 s. The scale bar is 5 mm. (d) Images of the $\pm1^{st}$ diffracted order switching between vortex light and Gaussian light under UV light irradiation based on the diagonal bending light-activated film FPG. From top to bottom, the UV light is irradiated 0 s, 4 s, 8 s, 12 s, 15 s. The scale bar is 5 mm. The incident light is linearly polarized with wavelengths of 633 nm, 532 nm, and 457 nm, respectively. The diffraction spots are captured at 70 cm.

Similarly, akin to the light-activated film FPG with a 50 μm period and a +2 topological charge, the light-activated film FPG with a period of 30 μm and a topological charge of +4 is also demonstrated the reversible switching between $\pm1^{st}$ order vortex light and Gaussian light.